1 Supplementary material

S1.1 AREBO Forward Kinematics

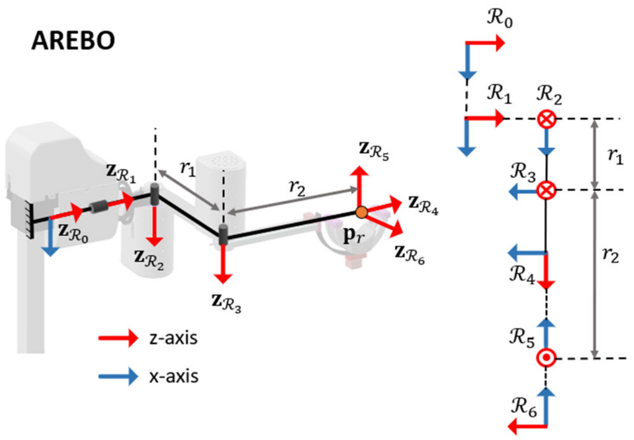

DH Parameters

	θ_i	a_i	d_i	α_i
1	θ_1	0	0	0
2	θ_2	0	0	$\frac{\pi}{2}$
3	$\theta_3 + \frac{\pi}{2}$	r_1	0	0
4	θ_4	0	r_2	$\frac{\pi}{2}$
5	$\theta_5 - \frac{\pi}{2}$	0	0	$\frac{\pi}{2}$
6	θ_6	0	0	$-\frac{\pi}{2}$

Figure S1. AREBO's 6 DOF kinematic chain with its DH parameters. The three proximal DOF $(\mathcal{R}_1, \mathcal{R}_2, \mathcal{R}_3)$ are actuated and control the 3D position of the robot's endpoint attached to the arm and the three distal unactuated DOF $(\mathcal{R}_4, \mathcal{R}_5, \mathcal{R}_6)$ help the robot to self-align to the orientation of the arm; these three DOF form a spherical joint about the robot's endpoint $\mathbf{p}_r$.

Forward kinematics computes the robot's endpoint position and orientation given the joint angles and DH parameters.

The homogenous transformation matrices between subsequent reference frames are given by:

$$\mathbf{T}_{\mathcal{R}_1}^{\mathcal{R}_0} = \begin{bmatrix} c_1 & -s_1 & 0 & 0 \\ s_1 & c_1 & 0 & 0 \\ 0 & 0 & 1 & 0 \\ 0 & 0 & 0 & 1 \end{bmatrix}, \mathbf{T}_{\mathcal{R}_2}^{\mathcal{R}_1} = \begin{bmatrix} c_2 & -s_2 & 0 & 0 \\ 0 & 0 & 1 & 0 \\ -s_2 & -c_2 & 0 & 0 \\ 0 & 0 & 0 & 1 \end{bmatrix}, \mathbf{T}_{\mathcal{R}_3}^{\mathcal{R}_2} = \begin{bmatrix} -s_3 & -c_3 & 0 & r_1 \\ c_3 & -s_3 & 0 & 0 \\ 0 & 0 & 1 & 0 \\ 0 & 0 & 0 & 1 \end{bmatrix}$$

$$\mathbf{T}_{\mathcal{R}_4}^{\mathcal{R}_3} = \begin{bmatrix} c_4 & -s_2 & 0 & 0 \\ 0 & 0 & -1 & -r_2 \\ s_4 & c_4 & 0 & 0 \\ 0 & 0 & 0 & 1 \end{bmatrix}, \mathbf{T}_{\mathcal{R}_5}^{\mathcal{R}_4} = \begin{bmatrix} s_5 & c_5 & 0 & 0 \\ 0 & 0 & -1 & 0 \\ -c_5 & s_5 & 0 & 0 \\ 0 & 0 & 0 & 1 \end{bmatrix}, \mathbf{T}_{\mathcal{R}_6}^{\mathcal{R}_5} = \begin{bmatrix} c_6 & -s_6 & 0 & 0 \\ 0 & 0 & 1 & 0 \\ -s_5 & -c_6 & 0 & 0 \\ 0 & 0 & 0 & 1 \end{bmatrix}$$

The position and orientation of the endpoint is given by:

$$\mathbf{T}_{\mathcal{R}_6}^{\mathcal{R}_0} = \mathbf{T}_{\mathcal{R}_1}^{\mathcal{R}_0} \cdot \mathbf{T}_{\mathcal{R}_2}^{\mathcal{R}_1} \cdot \mathbf{T}_{\mathcal{R}_3}^{\mathcal{R}_2} \cdot \mathbf{T}_{\mathcal{R}_4}^{\mathcal{R}_3} \cdot \mathbf{T}_{\mathcal{R}_5}^{\mathcal{R}_4} \cdot \mathbf{T}_{\mathcal{R}_6}^{\mathcal{R}_5}$$

Since θ_6 is not measured, it is assumed to be zero,

$$\mathbf{T}_{\mathcal{R}_6}^{\mathcal{R}_0} = \begin{bmatrix} \mathbf{R}_{\mathcal{R}_6}^{\mathcal{R}_0} & \mathbf{p}_{\mathbf{r}}^{\mathcal{R}_0} \\ \mathbf{0} & 1 \end{bmatrix}$$

where,

$$\mathbf{R}_{\mathcal{R}_6}^{\mathcal{R}_0} = \begin{bmatrix} -s_1 s_4 s_5 - c_1(c_{23}c_5 + c_4 s_{23} s_5) & -c_4 s_1 + c_1 s_{23} s_4 & -c_5(c_1 c_4 s_{23} + s_1 s_4) + c_1 c_{23} s_5 \\ -c_{23} c_5 s_1 + (-c_4 s_1 s_{23} + c_1 s_4) s_5 & c_1 c_4 + s_1 s_{23} s_4 & -c_4 c_5 s_1 s_{23} + c_1 c_5 s_4 + c_{23} s_1 s_5 \\ c_5 s_{23} - c_{23} c_4 s_5 & c_{23} s_4 & -c_{23} c_4 c_5 - s_{23} s_5 \end{bmatrix}$$

$$\mathbf{p}_r^{\mathcal{R}_0} = \begin{bmatrix} c_1(r_1 c_1 + r_2 c_{23}) \\ s_1(r_1 c_1 + r_2 c_{23}) \\ -r_1 s_1 - r_2 s_{23} \end{bmatrix}$$

where,

$s_{i_1 i_2 \cdots i_n} = \sin(\theta_{i_1} + \theta_{i_2} + \cdots + \theta_{i_n})$ and $c_{i_1 i_2 \cdots i_n} = \cos(\theta_{i_1} + \theta_{i_2} + \cdots + \theta_{i_n})$

S1.2 AREBO Inverse Kinematics

Inverse kinematics is used to find the robot's joint angles given the position and orientation of the endpoint. The position of the end point of the robot is given by:

$$\mathbf{p}_r^{\mathcal{R}_0} = \begin{bmatrix} p_{r,x} \\ p_{r,y} \\ p_{r,z} \end{bmatrix} = \begin{bmatrix} \cos\theta_1 \left(r_1 \cos\theta_2 + r_2 \cos(\theta_2+\theta_3)\right) \\ \sin\theta_1 \left(r_1 \cos\theta_2 + r_2 \cos(\theta_2+\theta_3)\right) \\ -r_1 \sin\theta_2 - r_2 \sin(\theta_2+\theta_3) \end{bmatrix}$$

Squaring and adding the terms,

$$p_{r,x}{}^2 + p_{r,y}{}^2 + p_{r,z}{}^2 = r_1{}^2 + r_2{}^2 + 2r_1 r_2 \cos\theta_3$$

Rewriting,

$$2r_1 r_2 \cos\theta_3 + (r_1{}^2 + r_2{}^2) - (p_{r,x}{}^2 + p_{r,x}{}^2 + p_{r,x}{}^2) = 0$$

$$\theta_3 = -\cos^{-1}\frac{(p_{r,x}{}^2 + p_{r,y}{}^2 + p_{r,z}{}^2) - (r_1{}^2 + r_2{}^2)}{2r_1 r_2}$$

The z-coordinate of the robot's endpoint is given by:

$$p_{r,z} = -r_1 \sin\theta_2 - r_2(\sin\theta_2 \cos\theta_3 + \sin\theta_3 \cos\theta_2)$$

$$(r_2 \sin\theta_3)\cos\theta_2 + (r_2\cos\theta_3)\sin\theta_2 + p_{r,z} + r_1 \sin\theta_2 = 0$$

Since θ_3 is known, the above trigonometric equation is solved by the procedure explained in section 1.3 to find θ_2.

Let, the orientation of the endpoint be:

$$\mathbf{R}_{\mathcal{R}_6}^{\mathcal{R}_0} = \begin{bmatrix} r_{11} & r_{12} & r_{13} \\ r_{21} & r_{22} & r_{23} \\ r_{31} & r_{32} & r_{33} \end{bmatrix}$$

θ_4 is calculated by solving the following trigonometric equation:

$$(\cos\theta_1)\cos\theta_4 + (\sin\theta_1 \sin(\theta_2+\theta_3))\sin\theta_4 - r_{22} = 0$$

Finally, θ_5 is obtained by solving the equation:

$$(\sin(\theta_2+\theta_3))\cos\theta_5 - \ (\cos(\theta_2+\theta_3)\cos\theta_4)\sin\theta_4 - r_{31} = \ 0$$

The above equations are of the form $a\cos\beta + b\sin\beta + c = 0$ and are solved by procedure explained in section S1.3.

S1.3 Solving equation of the form $a\cos\beta + b\sin\beta + c = 0$

$$a\cos\beta + b\sin\beta + c = 0$$

Substituting,

$$\cos\beta = \frac{1 - \left(\tan\frac{\beta}{2}\right)^2}{1 + \left(\tan\frac{\beta}{2}\right)^2} = \frac{1-t^2}{1+t^2}$$

$$\sin\beta = \frac{2\tan\frac{\beta}{2}}{1 + \left(\tan\frac{\beta}{2}\right)^2} = \frac{2t}{1+t^2}$$

And rewriting,

$$a\frac{1-t^2}{1+t^2} + b\frac{2t}{1+t^2} + c = 0$$

$$(c-a)t^2 + 2bt + (c+a) = 0$$

Solving for β,

$$t = \tan\frac{\beta}{2} = \frac{-b \pm \sqrt{a^2 + b^2 - c^2}}{(c-a)}$$

$$\beta = 2\tan\left(\frac{-b \pm \sqrt{a^2 + b^2 - c^2}}{(c-a)}\right)$$

S1.4 Arm Forward Kinematics

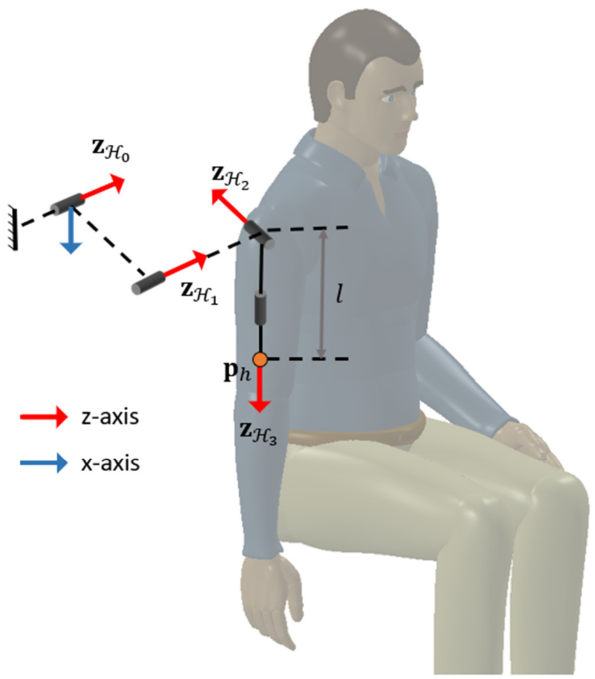

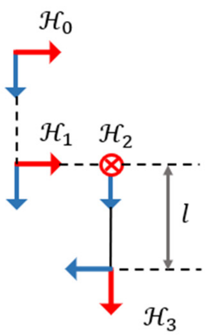

DH Parameters

	$\boldsymbol{\theta_i}$	$\boldsymbol{a_i}$	$\boldsymbol{d_i}$	$\boldsymbol{\alpha_i}$
1	0	0	0	ψ_x
2	ϕ_1	0	0	0
3	$\phi_2 + \frac{\pi}{2}$	l	0	$-\frac{\pi}{2}$
4	ϕ_3	0	0	$\frac{\pi}{2}$

Figure S2. Details of the three-DOF kinematic chain of the shoulder joint. The endpoint of the arm is at $\mathcal{H}_3$ at a distance l from its origin $\mathcal{H}_0$. The movements at the shoulder joint associated with the generalized coordinates of the arm are: ϕ_1 – flexion extension, ϕ_2 – abduction-adduction, ϕ_3 – internal external rotation

The homogenous transformation matrices between the reference frames are given by:

$$\mathbf{T}_{\mathcal{H}_0}^{\mathcal{R}_0} = \begin{bmatrix} 1 & 0 & 0 & x_{\mathcal{H}_0} \\ 0 & c_{\psi_x} & -s_{\psi_x} & y_{\mathcal{H}_0} \\ 0 & s_{\psi_x} & c_{\psi_x} & z_{\mathcal{H}_0} \\ 0 & 0 & 0 & 1 \end{bmatrix}, \mathbf{T}_{\mathcal{H}_2}^{\mathcal{H}_1} = \begin{bmatrix} c_1 & -s_1 & 0 & 0 \\ s_1 & c_1 & 0 & 0 \\ 0 & 0 & 1 & 0 \\ 0 & 0 & 0 & 1 \end{bmatrix},$$

$$\mathbf{T}_{\mathcal{H}_3}^{\mathcal{H}_2} = \begin{bmatrix} -s_2 & -c_2 & 0 & 0 \\ 0 & 0 & 1 & 0 \\ -c_2 & -s_2 & 0 & 0 \\ 0 & 0 & 0 & 1 \end{bmatrix}, \mathbf{T}_{\mathcal{H}_3}^{\mathcal{H}_2} = \begin{bmatrix} c_3 & -s_3 & 0 & 0 \\ 0 & 0 & -1 & l \\ s_3 & c_3 & 0 & 0 \\ 0 & 0 & 0 & 1 \end{bmatrix}$$

The position and orientation of the end point is found by:

$$\mathbf{T}_{\mathcal{H}_3}^{\mathcal{R}_0} = \mathbf{T}_{\mathcal{H}_0}^{\mathcal{R}_0} \cdot \mathbf{T}_{\mathcal{H}_2}^{\mathcal{H}_1} \cdot \mathbf{T}_{\mathcal{H}_3}^{\mathcal{H}_2} \cdot \mathbf{T}_{\mathcal{H}_3}^{\mathcal{H}_2}$$

As AREBO only supports two DOF movements of the arm, $\phi_3 = 0$,

$$\mathbf{T}_{\mathcal{H}_3}^{\mathcal{R}_0} = \begin{bmatrix} \mathbf{R}_{\mathcal{H}_3}^{\mathcal{R}_0} & \mathbf{p}_h^{\mathcal{R}_0} \\ \mathbf{0} & 1 \end{bmatrix}$$

$$\mathbf{R}_{\mathcal{H}_3}^{\mathcal{R}_0} = \begin{bmatrix} -c_1 s_2 & -s_2 & c_1 c_2 \\ -c_{\psi_x} s_2 s_1 + c_2 s_{\psi_x} & c_1 c_{\psi_x} & c_2 c_{\psi_x} s_1 + s_2 s_{\psi_x} \\ -c_1 c_{\psi_x} - s_2 s_1 s_{\psi_x} & c_1 s_{\psi_x} & -c_{\psi_x} s_2 + c_2 s_1 s_{\psi_x} \end{bmatrix}$$

$$\mathbf{p}_h^{\mathcal{R}_0} = \begin{bmatrix} x_{\mathcal{H}_0} + l c_1 c_2 \\ y_{\mathcal{H}_0} + l c_{\psi_x} c_2 s_1 + l s_2 s_{\psi_x} \\ z_{\mathcal{H}_0} - l c_{\psi_x} s_2 + l c_2 s_1 s_{\psi_x} \end{bmatrix}$$

where,

$s_{i_1 i_2 \cdots i_n} = \sin\left(\phi_{i_1} + \phi_{i_2} + \cdots + \phi_{i_n}\right)$ and $c_{i_1 i_2 \cdots i_n} = \cos\left(\phi_{i_1} + \phi_{i_2} + \cdots + \phi_{i_n}\right)$

S1.5 Arm Inverse Kinematics

Let the orientation of the arm with respect to the robot's base reference frame $\mathcal{R}_0$ be:

$$\mathbf{R}_{\mathcal{H}_3}^{\mathcal{R}_0} = \begin{bmatrix} h_{11} & h_{12} & h_{13} \\ h_{21} & h_{22} & h_{23} \\ h_{31} & h_{32} & h_{33} \end{bmatrix}$$

$$\phi_1 = \cos^{-1}\left(\frac{h_{22}}{\cos \psi_x}\right)$$

$$\phi_2 = -\sin^{-1} h_{12}$$

S1.6 Optimization

The first step in the design of the robot is the calculation of the link lengths. The link lengths were optimized with two objectives:

1. Maximize the workspace of the arm ($\mathcal{W}^a$) that is reachable by AREBO.
2. Maximize the manipulability along the plane orthogonal to the arm.

The objective function $O(r_1, r_2)$ written as a combination of these two objectives is defined as:

$$O(r_1, r_2) = \frac{1}{2}\left(O_w(r_1, r_2) + O_M(r_1, r_2)\right)$$

where $O_w(r_1, r_2)$ and $O_M(r_1, r_2)$ are the workspace and manipulability components of the objective function.

Workspace of the Arm

The workspace of the arm is decided by the position of the human joint $\mathcal{H}_0$ with respect to the robot's base reference frame $\mathcal{R}_0$, the distance of AREBO attachment from the human joint l and the trunk rotation ψ_x and the range of the joint angles ϕ_1, ϕ_2. The entire workspace is divided into discrete numbers of points based on the parameter combinations given in Table S1.

Table S1. Parameter values and range for the coarse and fine search used in the optimization of the robot link lengths. CS – coarse search, FS – fine search, l – distance between human joint and AREBO's attachment point, $\boldsymbol{o}_{\mathcal{H}_0}^{\mathcal{R}_0} = [o_x \quad o_y \quad o_z]^T$ is the origin of the human joint and ψ_x is the rotation of the human about $x_{\mathcal{H}_0}$ axis.

Parameter		Values (cm)	No of values
r_1	CS	{20, 22, ...,50}	16
	FS	{33.1, 33.2, ..., 34.9}	19
r_2	CS	{20, 22, ...,50}	16
	FS	{37.1, 37.2, ..., 38.9}	19
l		{15, 17.5, 20}	3
o_x , o_y		{-10, 0, 10}	3
o_z		{20, 30, 40}	3
ψ_x(deg)		{-30, 0, 30}	3

Workspace component $\boldsymbol{O_w(r_1, r_2)}$

Each point in the workspace of the arm is checked for its reachability with AREBO. A point is considered reachable if the AREBO's joint angles $\boldsymbol{\theta}$ yielded from its inverse kinematics are real and the angles are within the range:

$$-135° \leq \theta_1 \leq 0°$$
$$-45° \leq \theta_2 \leq 45°$$
$$-135° \leq \theta_3 \leq -45°$$
$$-45° \leq \theta_4 \leq 45°$$
$$-45° \leq \theta_5 \leq 45°$$

These constraints are applied to avoid regions closer to the singular configuration in AREBO. If the point is reachable, the reachability ($\eta_i(r_1, r_2, \boldsymbol{\theta})$) is denoted as 1, else it is 0. The workspace component $O_w(r_1, r_2)$ for a given r_1, r_2 is the average reachability in all points of the arm's workspace.

$$O_w(r_1, r_2) = \frac{\sum_{i=1}^{N} \eta_i\,(r_1, r_2, \boldsymbol{\theta})}{N}$$

$N \in \mathbb{N}$ is the total number of points in $\mathcal{W}^a$.

Manipulability component $O_w(r_1, r_2)$

Manipulability is defined as the ability of the robot to apply forces in different directions at a given joint space coordinate. In the case of AREBO, for safety reasons, it is required to apply forces only orthogonal to the arm (in the $\mathbf{x}_{\mathcal{R}_3}\,\mathbf{y}_{\mathcal{R}_3}$ plane).

The relationship between the forces applied by the robot orthogonal to the arm ($\mathbf{f}_{xy}$), along the axis of the arm ($\mathbf{f}_z$) and the actuator torques $\boldsymbol{\tau}^a$ is given by:

$$\mathbf{f}_{xy} = \mathbf{P}_{xy} \cdot \mathbf{J}(\boldsymbol{\theta})^{-T} \cdot \boldsymbol{\tau}^a$$
$$\mathbf{f}_z = \mathbf{P}_z \cdot \mathbf{J}(\boldsymbol{\theta})^{-T} \cdot \boldsymbol{\tau}^a$$

where $\mathbf{J}(\boldsymbol{\theta})$ is the Jacobian matrix of the robot as a function of the generalized coordinates $\boldsymbol{\theta}$.

$\mathbf{P}_{xy}, \mathbf{P}_z$ are the projection matrices to project the forces at the endpoint orthogonal to the arm and along the axis of the arm respectively.

Assuming the orientation of the endpoint is given by,

$$\mathbf{R}_{\mathcal{R}_6}^{\mathcal{R}_0} = [\mathbf{x}_{\mathcal{R}_6} \quad \mathbf{y}_{\mathcal{R}_6} \quad \mathbf{z}_{\mathcal{R}_6}]$$

The projection matrices can be calculated by the following relations:

$$\mathbf{P}_{\mathrm{xy}} = \mathbf{x}_{\mathcal{R}_6}\mathbf{x}_{\mathcal{R}_6}{}^T + \mathbf{y}_{\mathcal{R}_6}\mathbf{y}_{\mathcal{R}_6}{}^T$$
$$\mathbf{P}_{\mathrm{z}} = \mathbf{z}_{\mathcal{R}_6}\mathbf{z}_{\mathcal{R}_6}{}^T$$

The ratio of the ability to apply forces orthogonal to the arm and the ability to apply forces along the axis of the arm is given by,

$$\gamma_i(r_1, r_2, \boldsymbol{\theta}) = \frac{\|\mathbf{P}_z \cdot \mathbf{J}(\boldsymbol{\theta})^{-\mathbf{T}}\|_2}{\left\|\mathbf{P}_{xy} \cdot \mathbf{J}(\boldsymbol{\theta})^{-\mathbf{T}}\right\|_2}$$

The manipulability index $M_i(r_1, r_2, \boldsymbol{\theta})$ at a point in the $\mathcal{W}^a$ is 1 if $\gamma_i(r_1, r_2, \boldsymbol{\theta}) \geq 1$ else it is 0.

The manipulability component $O_w(r_1, r_2)$ for a given r_1, r_2 is the average of $M_i(r_1, r_2, \boldsymbol{\theta})$ across all points in the arm's workspace is,

$$O_M(r_1, r_2) = \frac{\sum_{i=1}^{N} M_i\,(r_1, r_2, \boldsymbol{\theta})}{N}$$

$N \in \mathbb{N}$ is the total number of points in $\mathcal{W}^a$.

S1.7 Schematic of the Hinge Joint at Unactuated DOF

Figure S3. A gives the schematic of the 6th and the 5th DOF. The circular platform on the 5th DOF has 12 bearings (figure S3. B) that are placed on its side and bottom. The eight bearings on the sides prevent translations about

$\mathbf{x}_{\mathcal{R}_6}$, $\mathbf{y}_{\mathcal{R}_6}$ and the four bearing in the does not allow translations along $\mathbf{z}_{\mathcal{R}_6}$ and rotations about $\mathbf{x}_{\mathcal{R}_6}$, $\mathbf{y}_{\mathcal{R}_6}$. Thus, this arrangement of 12 ball bearings allow only rotation about $\mathbf{z}_{\mathcal{R}_6}$ which forms the 6th DOF of the robot.

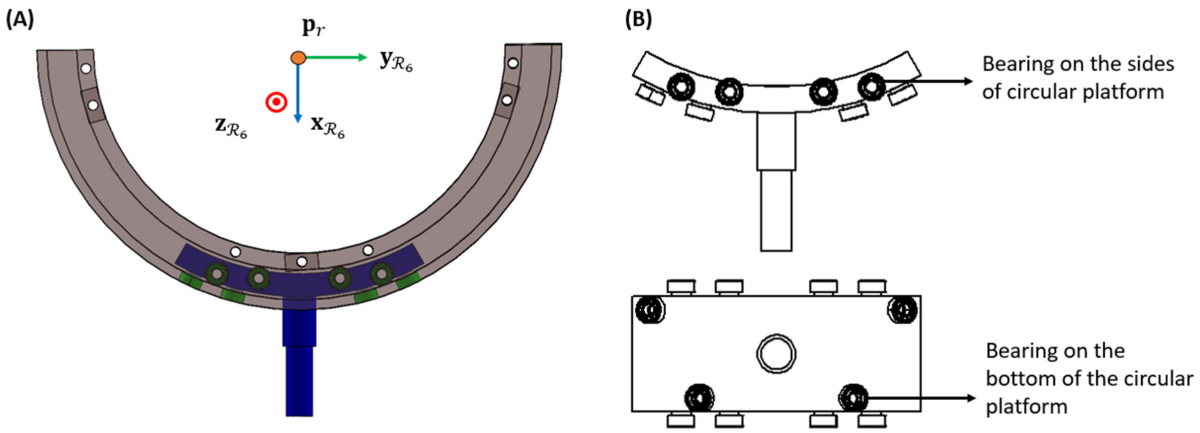

Figure S3. (A) Schematic of the unactuated DOF. (B) Front and Bottom view of the 5th DOF. $\mathbf{p}_r$ is the end point of AREBO and $\mathbf{x}_{\mathcal{R}_6}, \mathbf{y}_{\mathcal{R}_6}, \mathbf{z}_{\mathcal{R}_6}$ are the axis of the reference from $\mathcal{R}_6$.

Algorithm S1: Estimation of orientation

Algorithm 1: Estimation of orientation of human base frame with respect to the robot.

Let the record of the robot's endpoint position during the flexion-extension movements be $[\boldsymbol{p}_{r,x}[\boldsymbol{n}] \quad \boldsymbol{p}_{r,y}[\boldsymbol{n}] \quad \boldsymbol{p}_{r,z}[\boldsymbol{n}]]^T$, $\mathbf{0} \leq \boldsymbol{n} < \boldsymbol{N}$, where $\boldsymbol{n} \in \mathbb{Z}$ is the time index and $\mathbf{1} < \boldsymbol{N} \in \mathbb{Z}$ is the length of recorded data. The endpoint kinematics is computed from the joint angles of the robot.

Let the equation for the plane containing the flexion-extension movement be, $\boldsymbol{ax} + \boldsymbol{by} + \boldsymbol{c} = \boldsymbol{z}$. The robot's endpoint must satisfy this equation, which can be expressed as the following:

$$\begin{bmatrix} \boldsymbol{p}_{r,x}[\mathbf{0}] & \boldsymbol{p}_{r,y}[\mathbf{0}] & \mathbf{1} \\ \boldsymbol{p}_{r,x}[\mathbf{1}] & \boldsymbol{p}_{r,y}[\mathbf{1}] & \mathbf{1} \\ \vdots & \vdots & \vdots \\ \boldsymbol{p}_{r,x}[\boldsymbol{N}-\mathbf{1}] & \boldsymbol{p}_{r,y}[\boldsymbol{N}-\mathbf{1}] & \mathbf{1} \end{bmatrix} \begin{bmatrix} \boldsymbol{a} \\ \boldsymbol{b} \\ \boldsymbol{c} \end{bmatrix} = \begin{bmatrix} \boldsymbol{p}_{r,z}[\mathbf{0}] \\ \boldsymbol{p}_{r,z}[\mathbf{1}] \\ \vdots \\ \boldsymbol{p}_{r,z}[\boldsymbol{N}-\mathbf{1}] \end{bmatrix}$$

$$\mathbf{X} \cdot \mathbf{p} = \mathbf{z}$$

The algorithm for estimating the orientation parameter $\boldsymbol{\psi}_x$ is given below.

a) Estimate the parameters of the plane using the Moore-Penrose pseudoinverse, $\widehat{\mathbf{p}} = [\widehat{\boldsymbol{a}} \quad \widehat{\boldsymbol{b}} \quad \widehat{\boldsymbol{c}}]^T = \mathbf{X}^+ \cdot \mathbf{z}$. The normal to the plane is given by $\mathbf{n}_p = [\boldsymbol{a} \quad \boldsymbol{b} \quad -\mathbf{1}]^T$.

b) Find the angle between normal to plane and robot z-axis $\boldsymbol{\theta}_s = \pm \frac{\mathbf{1}}{\sqrt{\boldsymbol{a}^2+\boldsymbol{b}^2+\mathbf{1}}}$.

c) Find the vector $\mathbf{n}_s$ formed by rotating z-axis by angle $\boldsymbol{\theta}_s$,

$$\mathbf{n}_s = \begin{bmatrix} \mathbf{1} & \mathbf{0} & \mathbf{0} \\ \mathbf{0} & \cos\boldsymbol{\theta}_s & -\sin\boldsymbol{\theta}_s \\ \mathbf{0} & \sin\boldsymbol{\theta}_s & \cos\boldsymbol{\theta}_s \end{bmatrix} \begin{bmatrix} \mathbf{0} \\ \mathbf{0} \\ \mathbf{1} \end{bmatrix}$$

d) If, $\mathbf{n}_p^T \mathbf{n}_s \approx \mathbf{0} \Rightarrow \boldsymbol{\psi}_x = \boldsymbol{\theta}_s$, else $\boldsymbol{\psi}_x = -\boldsymbol{\theta}_s$.

Algorithm S2: Estimation of the human joint position and limb length

Algorithm 2 Finding initial human joint position $\mathbf{o}_{\mathcal{H}_0}^{\mathcal{R}_0}$ and distance between the joint to point of robot attachment $(\boldsymbol{l})$

- Let the robot joint angles recorded while the subject performs small random movements be: $\boldsymbol{\theta}[\boldsymbol{n}], \mathbf{0} \leq \boldsymbol{n} < \boldsymbol{N}$, where $\boldsymbol{n} \in \mathbb{Z}$ is the time index and $\boldsymbol{N} \in \mathbb{Z},\ \boldsymbol{N} > \mathbf{1}$ is the length of data available. The corresponding endpoint position and orientation are found by forward kinematics of AREBO and are given by $\mathbf{p}_r^{\mathcal{R}_0}[\boldsymbol{n}]$ and $\mathbf{R}_{\mathcal{R}_6}^{\mathcal{R}_0}[\boldsymbol{n}]$.

- Let the position of the human joint at $\boldsymbol{\mathcal{H}}_0$ be $\mathbf{o}_{\mathcal{H}_0}^{\mathcal{R}_0}$, then

$$\mathbf{o}_{\mathcal{H}_0}^{\mathcal{R}_0} = \mathbf{p}_r^{\mathcal{R}_0}[\boldsymbol{n}] - \boldsymbol{l} \cdot \mathbf{z}_{\mathcal{R}_6}^{\mathcal{R}_0}[\boldsymbol{n}]$$

- Rewriting,

$$\begin{bmatrix} \mathbf{I}_3 & \mathbf{z}_{\mathcal{R}_6}^{\mathcal{R}_0}[\boldsymbol{n}] \end{bmatrix} \begin{bmatrix} \mathbf{o}_{\mathcal{H}_0}^{\mathcal{R}_0} \\ \boldsymbol{l} \end{bmatrix} = \mathbf{p}_r^{\mathcal{R}_0}[\boldsymbol{n}]$$

- Substituting all the recorded points,

$$\begin{bmatrix} \mathbf{I}_3 & \mathbf{z}_{\mathcal{R}_6}^{\mathcal{R}_0}[\mathbf{0}] \\ \mathbf{I}_3 & \mathbf{z}_{\mathcal{R}_6}^{\mathcal{R}_0}[\mathbf{1}] \\ \vdots & \vdots \\ \mathbf{I}_3 & \mathbf{z}_{\mathcal{R}_6}^{\mathcal{R}_0}[\boldsymbol{N}-\mathbf{1}] \end{bmatrix} \begin{bmatrix} \mathbf{o}_{\mathcal{H}_0}^{\mathcal{R}_0} \\ \boldsymbol{l} \end{bmatrix} = \begin{bmatrix} \mathbf{p}_r^{\mathcal{R}_0}[\mathbf{0}] \\ \mathbf{p}_r^{\mathcal{R}_0}[\mathbf{1}] \\ \vdots \\ \mathbf{p}_r^{\mathcal{R}_0}[\boldsymbol{N}-\mathbf{1}] \end{bmatrix}$$

$$\mathbf{A}\mathbf{v} = \mathbf{b} \qquad \Rightarrow \quad \mathbf{v} = \mathbf{A}^{+}\mathbf{b}$$

$\mathbf{A}^{+}$ is Moore-Penrose inverse calculated as $\mathbf{A}^{+} = (\mathbf{A}^{T}\mathbf{A})^{-1}\mathbf{A}^{T}$

S1.8 AREBO Jacobian matrix

The Jacobian matrix relates the endpoint velocity $\dot{\mathbf{p}}_{\mathcal{R}_6}^{\mathcal{R}_0} \in \mathbb{R}^3$ in the task space to the angular velocities of the joints of AREBO, $\dot{\boldsymbol{\theta}} = [\dot{\theta}_1 \quad \dot{\theta}_2 \quad \dot{\theta}_3 \quad \dot{\theta}_4 \quad \dot{\theta}_5 \quad \dot{\theta}_6]^{T} \in \mathbb{R}^6$.

$$\dot{\mathbf{p}}_{\mathcal{R}_6}^{\mathcal{R}_0} = \begin{bmatrix} -s_1(r_1c_2 + r_2c_{23}) & -c_1(r_1s_2 + r_2s_{23}) & -r_2c_1s_{23} & 0 & 0 & 0 \\ c_1(r_1c_2 + r_2c_{23}) & s_1(r_1s_2 + r_2s_{23}) & r_2s_1s_{23} & 0 & 0 & 0 \\ 0 & r_1c_2 & r_2c_{23} & 0 & 0 & 0 \end{bmatrix} \begin{bmatrix} \dot{\theta}_1 \\ \dot{\theta}_2 \\ \dot{\theta}_3 \\ \dot{\theta}_4 \\ \dot{\theta}_5 \\ \dot{\theta}_6 \end{bmatrix}$$

$$\dot{\mathbf{p}}_{\mathcal{R}_6}^{\mathcal{R}_0} = \mathbf{J}(\boldsymbol{\theta}) \cdot \dot{\boldsymbol{\theta}}$$

where,

$s_{i_1 i_2 \cdots i_n} = \sin\left(\theta_{i_1} + \theta_{i_2} + \cdots + \theta_{i_n}\right)$ and $c_{i_1 i_2 \cdots i_n} = \cos\left(\theta_{i_1} + \theta_{i_2} + \cdots + \theta_{i_n}\right)$

S1.9 AREBO Gravity Compensation

The gravity compensation module of AREBO provides the actuator torques to hold the robot against gravity as a function of the joint angles $\boldsymbol{\theta}$. A simple calibration procedure is used to find this relationship by recording the torque sensor values at various combinations of $\boldsymbol{\theta}$. The procedure is automated by a PD position controller in the actuators of AREBO. The steps and range for the actuated joint angles are given in

Table S2, The steps and range of each actuated joint angle in the estimate of gravity compensation equations ($\boldsymbol{\tau}_g$) of AREBO.

Angle	Values (deg)	No. of values
θ_1	{0, -45, -90, -135, -90, -45, 0, 45, 0}	9
θ_2	{-45, 0, 45}	3
θ_3	{-45, 0, 45}	3

Thus, 81 data sets are recorded for fitting with the analytical equation of $\boldsymbol{\tau}_g$ that is derived from the potential energy of the robot V, where the overall potential energy is the sum of the individual potential energy of the individual links, as given below,

$$V = \sum_{i=1}^{5} w_i \left[\left(\prod_{j=0}^{i-1} \mathbf{R}_{\mathcal{R}_j}^{\mathcal{R}_{j+1}} \right) \mathbf{x}_i \right]_{2,1} \qquad , i \in \mathbb{N}, i = 1,2, \dots, 5$$

where,

- $\mathbf{x}_i$ are the coordinates of the centre of mass of link i in its local reference frame R_i
- w_i is the weight of link i,
- $[\cdot]_{2,1}$ is the element in the second row of column matrix A. This element is the y coordinate of the centre of mass in the global reference frame $\mathcal{R}_0$ and causes the change in the potential energy of the system.
- $\left(\prod_{j=0}^{i-1} \mathbf{R}_{\mathcal{R}_j}^{\mathcal{R}_{j+1}}\right) \mathbf{x}_i$ transforms the location of the centre of mass from frame $\mathcal{R}_i$ to $\mathcal{R}_0$.

The torque due to gravity $\tau_{g,i}$ at the i^{th} actuated DOF is given by,

$$\tau_{g,i} = -\frac{dV}{d\theta_i} \qquad , i \in \mathbb{N}, i = 1,2,3$$

Examining $\tau_{g,i}$, it can be rewritten in the form,

$$\tau_{g,i} = a_1 f_1(\boldsymbol{\theta}) + a_2 f_2(\boldsymbol{\theta}) + \cdots + a_n f_n(\boldsymbol{\theta})$$

where,

- a_x ($a_x \in \mathbb{R},\ x \in \mathbb{N},\ x = \{1,2, \dots, n\}$)are constants which are the product of the weight of the link and the centre of mass coordinates,
- $f_x(\boldsymbol{\theta})$ are trigonometric functions in joint coordinates $\boldsymbol{\theta}$.

The constants a_x are treated as unknowns and a linear fit is made in Mathematica with recorded encoder and torque sensor data sets to determine $\boldsymbol{\tau}_g$. The equations are then exported to Arduino to set the feedforward current to the actuators for gravity compensation.

S1.10 Gains of AREBO Controller

The high-level controller in AREBO sets the interaction force applied by the robot on the user. It uses a PD controller with gains as given below:

1st Joint	$K_{1,1} = \begin{cases} 4, \tau_1^{int} > 0 \\ 2, \tau_1^{int} < 0 \end{cases}, K_{1,2} = 2$
2nd Joint	$K_{2,1} = 3, K_{2,2} = 2$
2nd Joint	$K_{3,1} = 3, K_{3,2} = 2$

S1.11 Human Limb Model

A simple calibration procedure was employed to estimate the human joint torques due to the weight of the human limb as a function of the human limb angle $\boldsymbol{\phi}$. This calibration procedure is done after completing the estimation of the human limb length l and the orientation ψ_x of the human base frame. For estimating the weight of the upper arm, a flexion-extension movement is imposed on the human shoulder joint while the joint angle and torques of AREBO are recorded. This data is used to estimate the human limb joint angles and the torque required to hold the upper arm against gravity, and the interaction force is measured. The position controller of AREBO is activated to take the arm to various flexion angles (ϕ_1) and hold for 2 seconds to record the static torque at the joints of AREBO. The torque due to the weight of the arm is recorded as, $\boldsymbol{\tau}_{int} = [\tau_{int,1} \quad \tau_{int,2} \quad \tau_{int,3}]^T$is calculated as:

$$\boldsymbol{\tau}_{int} = \boldsymbol{\tau}_r - \boldsymbol{\tau}_g$$

where,

$\boldsymbol{\tau}_r$ is the torque read at the torque sensors,

$\boldsymbol{\tau}_g$ is the torque due to the weight of the links of the robot.

The interaction torque is transformed to the human base reference frame to find the human joint torques $\boldsymbol{\tau}_h = [\tau_{h,1} \quad \tau_{h,2} \quad \tau_{h,3}]^{\boldsymbol{T}}$.

$$\boldsymbol{\tau}_h = \mathbf{R}_{\mathcal{R}_0}^{\mathcal{H}_0} . \boldsymbol{\tau}^{int}$$

Only $\tau_{h,1}$ varies with the joint angles as the arm performs flexion extension and $\tau_{h,2}, \tau_{h,3}$ are negligible. Assuming the center of mass of the arm lies along the axis of the arm, a linear fit was made in Mathematica with the equation, $\tau_{h,1} = \tau_{max} \sin \phi_1$ to find the constant τ_{max} and hence the weight torque $\tau_{h,1}$ at the shoulder as a function of the flexion angle ϕ_1.

The gravitational torque to hold the arm as a function of the joint angles ϕ_1, ϕ_2 is given by:

$$\boldsymbol{\tau}_{\mathrm{h}} = \begin{bmatrix} \tau_{max} \sin \phi_1 \cos \phi_2 \\ \tau_{max} \sin \phi_2 \cos \phi_1 \\ 0 \end{bmatrix}$$

S1.12 SJM Joint Actuation and Sensing

The same Teensy 4.1 microcontroller is used to control both SJM and AREBO. Like AREBO, PWM lines from the microcontroller to the motor controllers are used to vary the torque in the actuators of SJM and four digital lines (channel A, channel B for each encoder) are used to read the encoders. HX711 load cell amplifiers are connected to each torque sensor and two digital lines from the amplifier are used to obtain the torque at the joints of SJM.

Table S3. Specification of actuators and torque sensors used in SJM. Actuators from Maxon International Ltd. and torque sensors from Forsentek Co., Ltd. An Escon 70/10 ec controller is used to control flexion/extension DOF and an Escon 36/3 EC controller is used for abduction/adduction DOF.

	Motor	Gearbox	Torque Sensor	Encoder
1st Joint	EC Flat 90, Nominal torque – 0.953 Nm, part no. 607950	GP 52 C, Gear ratio: 53:1, part no. 223090	FTHC, Range - 40 Nm	MILE, 4096 CPT, part no. 651168
2nd Joint	EC Flat 45, Nominal torque – 0.128Nm, part no. 397172	GP 42 C, Gear ratio 43:1, part no. 203120	FTHB, Range - 5 Nm	MILE, 2048 CPT, part no. 462005

S1.13 Closed Loop Bandwidth

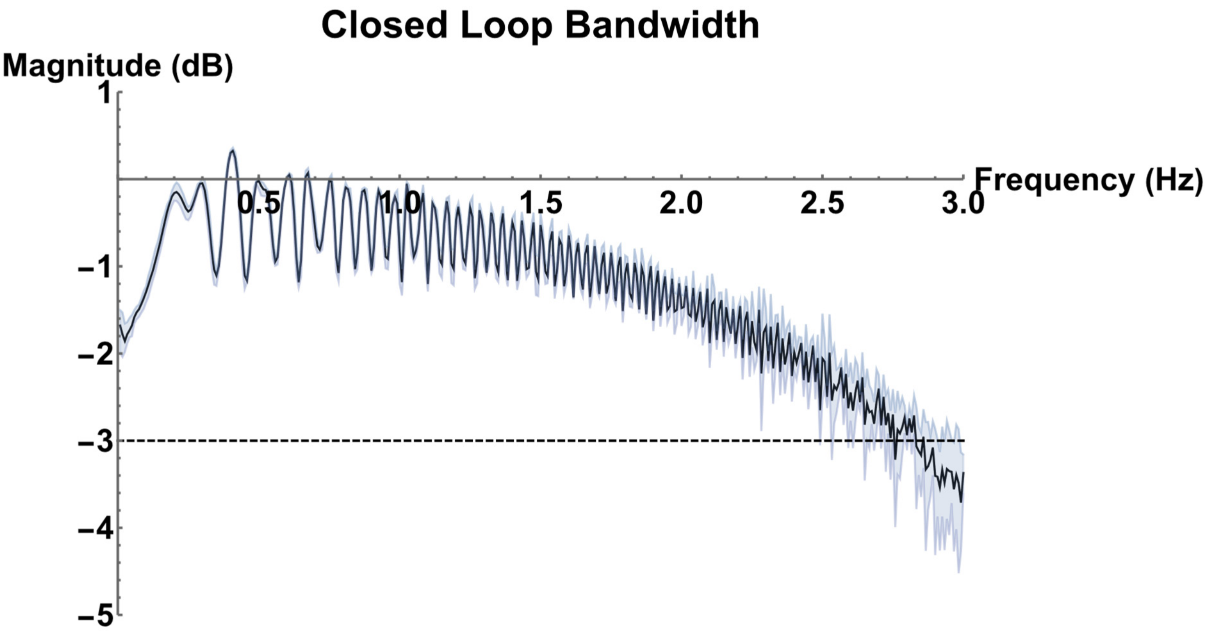

Figure S4. Closed loop bandwidth for the actuator used in 2nd DOF.

To identify the torque controller bandwidth the output shaft of the actuator was fixed after attaching a torque sensor in series to it. Input torque was set by sending digital signals from Teensy 4.1 microcontroller to the Maxon motor controller, and the torque sensor reading was recorded as the output. A chirp signal with amplitude 15 Nm, 0 to 3 Hz sweep over 120 seconds was used to vary the input torque. The magnitude spectrum of the closed loop torque controller is calculated as the ratio of the average FFTs of the input and the output torque profiles. A 3 dB cutoff was used in the calculation of bandwidth. Figure S4 shows the results for the 2nd actuator and the bandwidth in this case is 2.74 Hz. The experiment was repeated for other actuators as well and similar results were obtained.

S1.14 Details of SJM controller

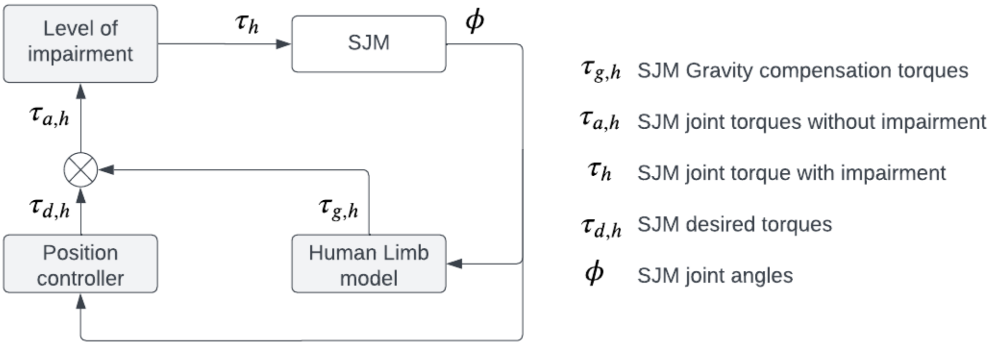

Figure S5. Block diagram of the controller implemented in SJM.

The SJM was designed to be a 2 DOF kinematic and dynamic model of the human arm that can be trained by AREBO. The various blocks in the controllers implemented in SJM illustrated in Figure S5 are:

a) **Low-level current control loop** – The Maxon motor controllers (Escon 70/10 ec) implement the current control at the lowest level based on the PWM signals sent by the Teensy 4.1 microcontroller.
b) **Human limb model** – The module computes the SJM joint torques to hold it against gravity at various joint space coordinates of SJM.
c) **High-level position control loop** – The position controller moves SJM to the desired joint space coordinates depending on the control mode that is tested (zero torque or adaptive weight support mode).
d) **Level of impairment** – This block simulates the weakness in the arm by multiplying the desired torque from the position controller by a factor $1 - \xi$, $(\xi \in \mathbb{R}, 0 \leq \xi \leq 1)$. $\xi = 0$, implies there is no impairment in the arm and $0 < \xi \leq 1$ denotes the presence of arm impairments.

S1.15 Effects of Shoulder Abduction Joint Angle on the Estimation of the Orientation of the Human Base Frame.

In practical scenarios, it is not possible to perform a pure flexion-extension movement for the calibration procedure to find ψ_x. To study the effects of these real-life movements on the accuracy of the human joint angles estimated by AREBO, randomly varying abduction movement, (ϕ_2) was imposed in SJM while it performs the flexion-extension movement (ϕ_1). Three scenarios were considered in the experiment: 1) ϕ_2 is almost zero denoting pure flexion movements $(\phi_2 \cong 0)$, 2) ϕ_2 varying between $\pm 5°$ $(-5° \leq \phi_2 \leq 5°)$, 3) ϕ_2 varying between $\pm 10°$ $(-10° \leq \phi_2 \leq 10°)$, as shown in Figure S6A. The ψ_x estimated in the three cases is then used to individually estimate the joint angles for the same randomly varying polysine movement performed by SJM. During this random movement, ϕ_1 varied between 0 to 90 degrees and ϕ_2 varied between -30 and +30 degrees.

The encoder values of SJM are considered as ground truth to calculate the error in AREBO's estimates of the joint angles.

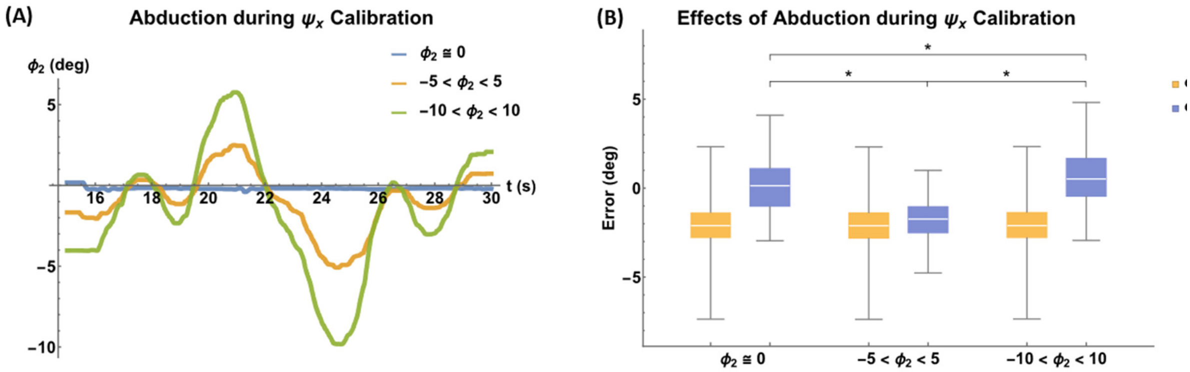

Figure S6. (A) Randomly varying Abduction during the calibration procedure to find ψ_x. The blue curve is the has near zero ϕ_2 representing pure flexion extension movement. The yellow and green curves depict the randomly varying ϕ_2 between $\pm 5°$ and $\pm 10°$ respectively. (B) Errors in the joint angle estimated by AREBO due to the change in ϕ_2 during ψ_x calibration. e_f – error in flexion, e_a- error in abduction, * - significant difference between the groups (p < 0.05 in one way ANOVA).

Results of the angle estimates in the three cases show that the flexion angle is independent of the value of ψ_x estimated and there was no significant difference between the groups (p>0.05 in one-way ANOVA). The errors in abduction were significantly different (p<0.05 in one-way ANOVA). The absolute median errors were high in the case of flexion ($2.10°$) as compared to the error in abduction ($1.73°$).

S1.16 Error in Shoulder Angle Estimation Due to Fixed Trunk Assumption

Compensatory movements are often employed by stroke survivors with arm impairments and the shoulder joint position may not be fixed during these movements. The kinematic model of the shoulder joint used in the study does not take this into account and hence, a theoretical analysis is performed to evaluate the errors due to compensatory movements of the trunk on the human joint angle estimation error. A 5 DOF kinematic model of the trunk is used to simulate the conditions where the shoulder joints are not fixed as shown in Figure S7.
Let $\mathcal{B}_1 - \mathcal{B}_5$ be the reference frames that control the various movements of the trunk. $\mathcal{B}_1, \mathcal{B}_2, \mathcal{B}_3$ form a spherical joint at the base of the spine and $\mathcal{B}_4, \mathcal{B}_5$ form the sternoclavicular joint. If γ_i $(i \in 1,2,..,5)$ is the angle associated with the reference frame $\mathcal{B}_i$, the movement corresponding to each angle is as follows:

1. γ_1 – trunk flexion/extension
2. γ_2 – trunk lateral flexion/extension
3. γ_3 – trunk twist
4. γ_4 – shoulder protraction/retraction
5. γ_5 – shoulder elevation/depression

The five DOFs of the trunk together vary the position of the shoulder joint $\mathcal{H}_0$.

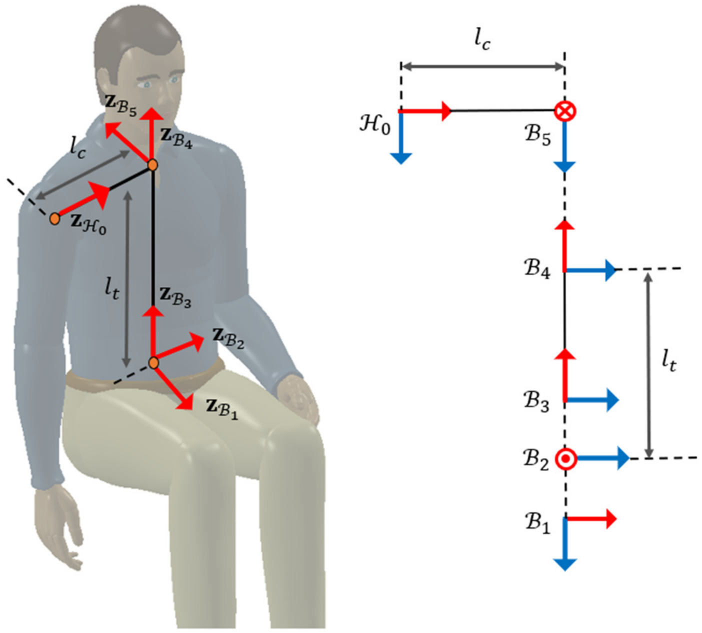

DH Parameters

	θ_i	a_i	d_i	α_i
1	γ_1	0	0	0
2	$\gamma_2 + \frac{\pi}{2}$	0	0	$\frac{\pi}{2}$
3	γ_3	$-l_t$	0	$\frac{\pi}{2}$
4	γ_4	0	0	0
5	$\gamma_5 + \frac{\pi}{2}$	0	0	$\frac{\pi}{2}$
6	0	$-l_c$	0	$-\frac{\pi}{2}$

Figure S7. Kinematic model of the trunk. The movements of the trunk are controlled by five reference frames $\mathcal{B}_1 - \mathcal{B}_5$ and l_t, l_c are the lengths of the trunk and clavicle. The kinematic chain of the trunk end at the shoulder joint with reference frame $\mathcal{H}_0$.

Evaluation of errors in human joint angles due to trunk movements

Random polysine trajectories of 20 seconds duration are generated in MATHEMATICA and are incorporated to all the angles of the trunk ($\gamma_1 - \gamma_5$ varying between $\pm 20°$) and the shoulder joint (ϕ_1 varying between $\pm 45°$, ϕ_2 varying between $0° - 45°$). The rotation of the human base frame with respect to the robot, ψ_x is assumed to be a constant value chosen randomly between $\pm 30°$. At each time instant, the point of attachment of the robot with human arm is calculated by the forward kinematics analysis of the 7DOF kinematic trunk-arm model. The human joint angle estimation algorithm is then invoked to calculate angles ϕ_1, ϕ_2 that will be estimated by AREBO, and the analysis is repeated 20 times.

Figure S8 shows the results of the errors in joint angle estimation algorithm due to trunk movements. The deviations of the shoulder joint coordinates during the random movements induced in the trunk are shown in Figure S8A. The plot in Figure S8B depicts the trajectories of the actual and estimated flexion (ϕ_1) and abduction (ϕ_2) angles. The (5^{th}, 95^{th} percentile) errors from the analysis are 1) $(-16.2°, 16.5°)$ for flexion and 2) $(-23.89°, 20.17°)$ for abduction. The variation of the errors in angles ϕ_1, ϕ_2 is illustrated by box plots in Figure S8C.

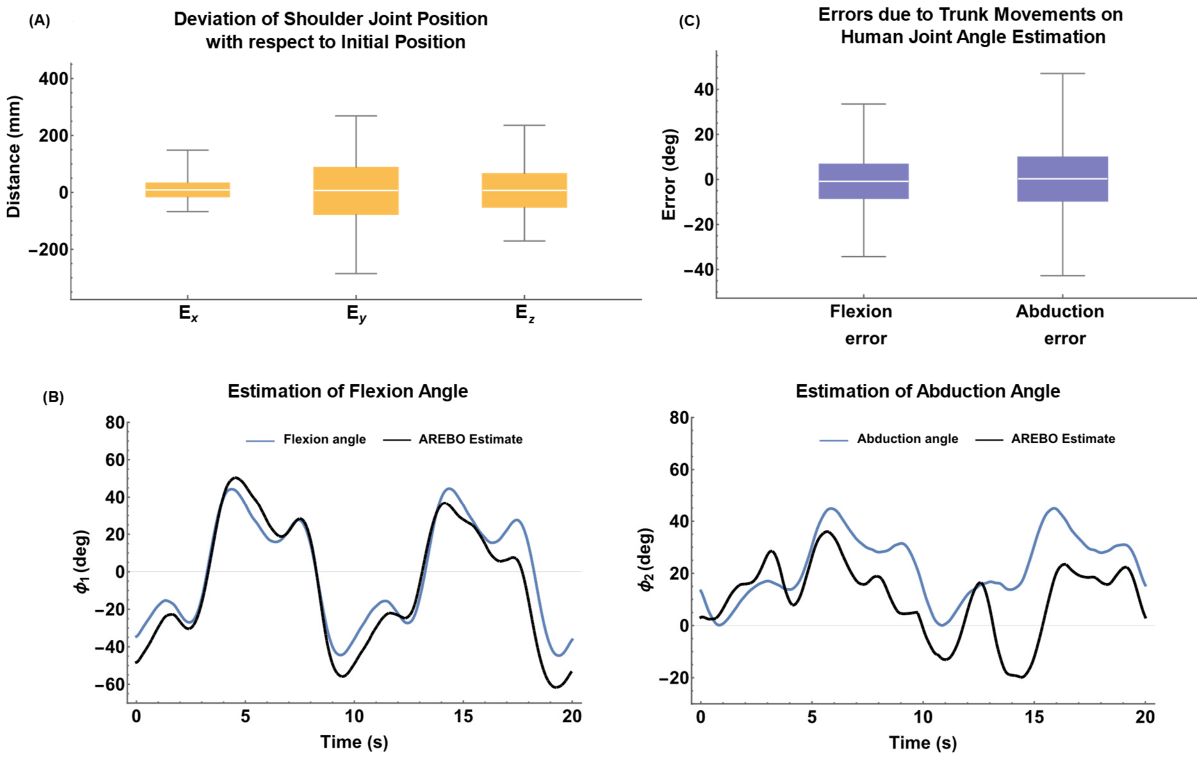

Figure S8. Effects of trunk movements on joint angle estimation algorithm. (A) Deviation of the position of the shoulder joint with respect to initial position due to trunk movements, $\mathbf{E} = [E_x \quad E_y \quad E_z]^T$ are deviations of the shoulder joint along $\mathbf{x}_{\mathcal{H}_0}, \mathbf{y}_{\mathcal{H}_0}, \mathbf{z}_{\mathcal{H}_0}$ axes respectively. (B) Actual angles of the shoulder and estimation from AREBO with the human joint angle estimation algorithm. (C) Distribution of the flexion and abduction errors in the 20 sets of random movements considered.